Manuscript

Chenyu Wang

May 26, 2025

1 Outline

- Intro to Drift Diffusion Model (DDM)
  - Formalization DDM
  - Reparameterization of DDM using Markov process and its connection to Neural circuit model
- Neural representation of decision variable x in DDM via Laplace / inverse Laplace transform
  - Representation of temporal history of events
  - From temporal past to any time-related variables through $\alpha(t) = dx/dt$
  - translational invariant property (bump & edge) of neural activity as a function of log evidence
- Formalization of the neural circuit model
  - Parameterization of the Edge / Bump attractor models
  - Customization of Synaptic Weights using different connectivity kernels
  - Illustration of edge-bump coupling dynamics
  - Calculation of the theoretical moving speed and use them to predict animal's behavior
- Application of the Neural circuit model
  - Given a set of DDM parameters inferred from the behavioral data, construct a corresponding neural circuit model
  - Evaluate the neural circuit model parameters from the ephy data

2 Methods

2.1 Drift Diffusion Model

We start with the one-dimensional drift diffusion model (DDM) with a symmetric absorbing boundary B. The decision variable x is governed by

$$dx = Adt + \sigma_W dW \tag{1}$$

where A is the drift rate and $\sigma_W dW$ is a Wiener process with scaling σ_W. The boundary B prevents $x(t)$ from evolving further (i.e., $dx = 0$ if $x(t) > B$). For simulation purposes, we approximate this continuous process with a discrete Markov random walk. Over a small time interval Δt, the decision variable increases by Δx with probability p or decreases by Δx with probability $1 - p$. We match the mean and variance of a single discrete step to those of the continuous process over the interval Δt:

$$\begin{aligned} \mu &= (2p - 1)\Delta x = v\Delta t \\ \sigma^2 &= 4\Delta x^2(1 - p)p = \sigma_W^2 \Delta t \end{aligned} \tag{2}$$

Solving this system, we represent p and Δa as:

$$\begin{aligned} \Delta x &= \sqrt{\sigma_W^2 \Delta t + (v\Delta t)^2} \\ p &= \frac{1}{2}(1 + \frac{v\Delta t}{\Delta x}) \end{aligned} \tag{3}$$

In the following section we will introduce an attractor neural circuit model that exactly represents the DDM model by encoding the Laplace transform of the decision variable a.

2.2 Laplace Transform of decision variable x

Let $F_s(t)$ describe the firing rate of a group of cells each with a positive value s. These cells update its current value by obeying the following differential equation,

$$\frac{dF_s(t)}{dt} = \alpha(t)[-sF_s(t) + f(t)] \tag{4}$$

If $\alpha(t) \equiv 1$ and we assume $f(t) = \delta(t - t_0)$ represents an event happening at time t_0, solving this differential equation,

$$F_s(t) = \int_{-\infty}^{t} e^{-s(t-t')}\delta(t' - t_0)dt' = e^{-s(t-t_0)} \tag{5}$$

This suggests that all cells together code a Laplace transform of the event time. Now consider $\alpha(t) = \frac{dx}{dt}$ where x is the decision variable. Further assume f is only a function of x. Applying the chain rule we find,

$$\frac{dF_s(x)}{dx} = -sF_s(x) + f(x) \tag{6}$$

Now assume $f(x) = \delta(x)$. Then similarly, we conclude that these cells together code a Laplace transform of the decision variable.

If we assume s values of all cells follow a geometric series,

$$s_n = s_0 a^{-(n-n_0)} \tag{7}$$

Then the solution of the system yields

$$F_n(x) = \exp(-s_0 a^{-(n-n_0)} x) \tag{8}$$

Notice if we consider $F_n(x)$ as a function of n and x, we have

$$F_(n + \delta n, x + \delta x) = F_n(n, x) \tag{9}$$

for some δn and δx. This suggests that the activity has translated across the population along the evidence x. In fact, the neural activities of all cells as a function of n form a translational edge, much like the translational "bump" in head direction cells that instantaneously tracks the animal's heading orientation.

2.3 Edge-bump Attractor Model

2.3.1 Network Dynamics

Our neural circuit model is composed of two neural populations, each of which forms a continuous attractor and interacts with each other to dynamically encode the decision variable. Similar to the tuning properties of head direction cells, neurons are indexed by their preferred evidence level $x \in [0, B]$, where B is the boundary of making a decision. The two populations are characterized by their response properties: bump neurons (first population) show peak firing rates at their preferred evidence level x, collectively forming a 'bump' as an attractor state. In contrast, edge neurons (second population) show the maximum slope (rate of change) in firing rate at their preferred evidence level x, collectively forming an 'edge' as an attractor state. Each of the two populations itself contains two subpopulations of neurons, one left-preferring population and one right-preferring population. We defined the dynamics of neurons as

$$\begin{aligned}\tau_B \frac{dU_{B,D}(x,t)}{dt} &= -U_{B,D}(x,t) + \int_{-1}^{1} dx' J_{BB}(x,x') r_{B,D}(x',t) + I_{EB,D}(x,t) + I^E_{\text{ext}}(x,t) \\ \tau_E \frac{dU_{E,D}(x,t)}{dt} &= -U_{E,D}(x,t) + \int_{-1}^{1} dx' J_{EE}(x,x') \tilde{r}_{E,D}(x',t) + I_{BE,D}(x,t)\end{aligned} \tag{10}$$

where $U_{B,D}$ and $U_{E,D}$ are the instantaneous synaptic inputs and $D \in \{L, R\}$. τ_B, τ_E are time constants. $r_{B,D}$ is the firing rate of bump neurons, and $\tilde{r}_{E,D}$ is the normalized firing rate of edge neurons ranging between -1 and 1. J_{BB} and J_{EE} are recurrent weights within bump and egde populations. I_{EB} and I_{BE} are inputs from edge neurons to bump and from bump neurons. I_{EB} and I_{BE} are the cross-population inputs (Edge-to-Bump and Bump-to-Edge, respectively).

2.3.2 Synaptic Weights

For both neural populations, we assume that the connection between neuron i and neuron j only depends on its difference in evidence space

$$J(x_i, x_j) \equiv K(x_i - x_j) \tag{11}$$

where K is the connectivity kernel.

Inspired by previous study on CANN model, we chose Gaussian interactions for the connectivity kernels of bump neurons,

$$J_{BB}(x,x') \equiv K_B(x - x') = \frac{1}{\sqrt{2\pi}a} \exp\left[-\frac{(x-x')^2}{2a^2}\right] \tag{12}$$

together with the neural nonlinearity given by the divisive normalization,

$$r_B(x,t) = \frac{U_B(x,t)^2}{1 + \rho \int_{-1}^{1} dx' U_B(x',t)^2} \tag{13}$$

where a defines the interaction width and ρ is the neural density. This CANN model is solvable: it holds a continuous Gaussian stationary states,

$$U(x|z) = U_0 \exp\left[-\frac{(x-z)^2}{4a^2}\right] \tag{14}$$

where the bump location z depends on the external input. In our simulation we applied a brief external stimulus to activate the bump neurons. The stimulus is Gaussian centered at 0 in evidence space,

$$I^E_{\text{ext}}(x,t) = \begin{cases} \exp\left(-\frac{x^2}{4a^2}\right), & t \le t_{\text{start}} \\ 0, & t > t_{\text{start}} \end{cases} \tag{15}$$

The connectivity kernel of edge neurons depends on the equilibrium shape of the edge as a function of x, $U^*_E(x)$, which is the desired solution of

$$U_E(x) = \int_{-1}^{1} dx' J_{EE}(x,x') \tilde{r}_E(x') \tag{16}$$

where we use the tanh nonlinearity

$$\tilde{r}_E(x') = \tanh(\sigma_E U_E(n)) \tag{17}$$

Discretizing the evidence space $x_n = n\Delta x$ ($n \in \mathbf{Z}$). Suppose the edge changes its sign at $n = m$ (i.e., $U_E(x_{m+1}) < 0$ and $U_E(x_m) > 0$). When $\sigma_E \to \infty$, the tanh nonlinearity reduces to a step function.

Therefore, we have

$$\begin{aligned} U_E^*(x_{n+1}) - U_E^*(x_n) &= \sum_{n'} [K_E(n+1-n') - K_E(n-n')] \tanh(\sigma_E U_E^*(x_{n'})) \\ &= \sum_{n'=-\infty}^{m} \Delta K_E(n-n') - \sum_{n'=m+1}^{\infty} \Delta K_E(n-n') \\ &= 2\sum_{n'=-\infty}^{m} \Delta K_E(n-n') \\ &= 2K_E(n-m+1) \end{aligned} \tag{18}$$

where we used the fact $\sum_{n=-\infty}^{\infty} \Delta K_E(n-n') = 0$. Let $\Delta x \to 0$, we have

$$K_E(\delta x) = \frac{1}{2} \frac{dU_E^*(x)}{dx}|_{x=\delta x+m-1} \tag{19}$$

If we assume that the edge neurons exactly encode the Laplace transform of the decision variable, i.e.,

$$U_E^*(x_n) = 2\exp\left[-\ln 2a^{-(x_n-x_0)}\right] - 1 \tag{20}$$

Then we have

$$K_E(\delta x) = (\ln 2)(\ln a)a^{-\delta x}2^{-a^{-\delta x}} \tag{21}$$

Alternatively, we can use the tanh function to approximate the activities of edge neurons,

$$U_E^*(x_n) = -\tanh(\sigma_E(x_n - x_0)) \tag{22}$$

This suggests

$$K_E(\delta x) = -\frac{\sigma_E}{2} \frac{1}{\cosh^2(\sigma_E \delta x)} \tag{23}$$

The use of the tanh function results in a symmetric connectivity kernel that depends exclusively on the distance between neurons in evidence space. Such symmetry is characteristic of continuous attractor networks, as is the case with the Gaussian kernel we used to construct the bump attractor, where recurrent excitatory connections are typically modeled as symmetric functions of network distance.

2.3.3 Communications Between Bump attractor and Edge Attractor

The neural circuit model dynamically tracks the evolution of decision variable states by continuously modulating the connectivity between edge and bump attractors in a reciprocal manner. Specifically, consider given times of left cues t_L and right cues t_R in a perceptual decision making task, we let

$$\begin{aligned} I_{EB,D}(x,t) &= c_E \frac{\partial}{\partial x} \tilde{r}_{E,D}(x,t) \\ I_{BE,D}(x,t) &= c_B \mathbf{1}_D(t) r_{B,D}(x,t) \end{aligned} \tag{24}$$

where $\mathbf{1}_D(t) = \begin{cases} 1, t \in t_D \\ 0, t \notin t_D \end{cases}$, $D = \{L, R\}$, and c_E, c_B controls the connection strength.

Initially, the bump and edge attractors are co-localized in the evidence space. When a cue from direction D arrives, $I_{BE,D}$ pushes the bump attractor toward D. At the same time, $I_{EB,D}(x,t)$ adds a bump-shaped input whose peak lies slightly ahead of the bump. This offset pulls the bump toward the edge attractor, allowing the two activity patterns to realign as the decision variable evolves.

2.4 Calculation of the theoretical edge/bump speed during the task

Assume the center of the bump is always anchored with the center of the edge. Suppose the edge moves to the right with speed v:

$$x_E^*(t) = \begin{cases} x_0, & t \le t_0, \\ x_0 + v(t - t_0), & t > t_0. \end{cases} \tag{25}$$

where x_E^* represents the center of the bump attractor. Correspondingly, the solution of the edge is:

$$\hat{U}_E(x,t) = \begin{cases} -\tanh(\sigma_1(x - x_0)), & t \le t_0, \\ -\tanh\Big(\sigma_1(x - x_0 - v(t - t_0))\Big), & t > t_0. \end{cases} \tag{26}$$

For $t > t_0$ we have:

$$\begin{aligned} \frac{d}{dt}\hat{U}_E(x_E^*(t),t) &= -\hat{U}_E(x_E^*(t),t) + \int_{x'} J_{EE}(x_E^*(t),x')\,\tilde{r}_E(x',t)dx' + c_B U_B(x_E^*,t) \\ &= c_B h_B \end{aligned} \tag{27}$$

where h_B is the bump height. From the assumption we have

$$\begin{aligned} \frac{d}{dt}\hat{U}_E(x_E^*(t),t) &= \Big(1 - \tanh^2\big(\sigma_1(n^* - n_0 - v(t - t_0))\big)\Big)\cdot \sigma_1 v \\ &= \sigma_1 v \end{aligned} \tag{28}$$

Comparing Eq. 25 and Eq. 26 we have

$$v = \frac{2c_B h_B}{\sigma_1} \tag{29}$$

This correspondence suggests a linear correlation between the parameter that controls the connection strength and the edge/bump speed.

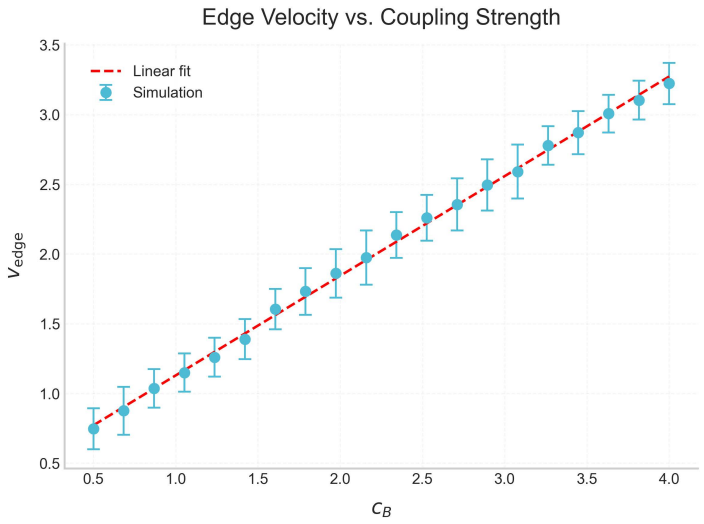

Figure 1: *Relationship between the edge velocity and the coupling strength* c_B In this simulation we use $A = 0.5$, $\sigma_W = 0.5$, $B = 0.8$. The simulated edge speed is defined as the averaged change of bump location within each trial. For each c_B we perform 10 times of simulation, each of which with different sets of observation cues.

3 Applications of the Neural Circuit Model

3.1 Mapping from the Edge-bump Attractors to the Drift Diffusion Model

In this section we demonstrate how it is possible to construct an attractor network that represents the decision variable in a standard DDM by accumulating evidence within and between neural populations.

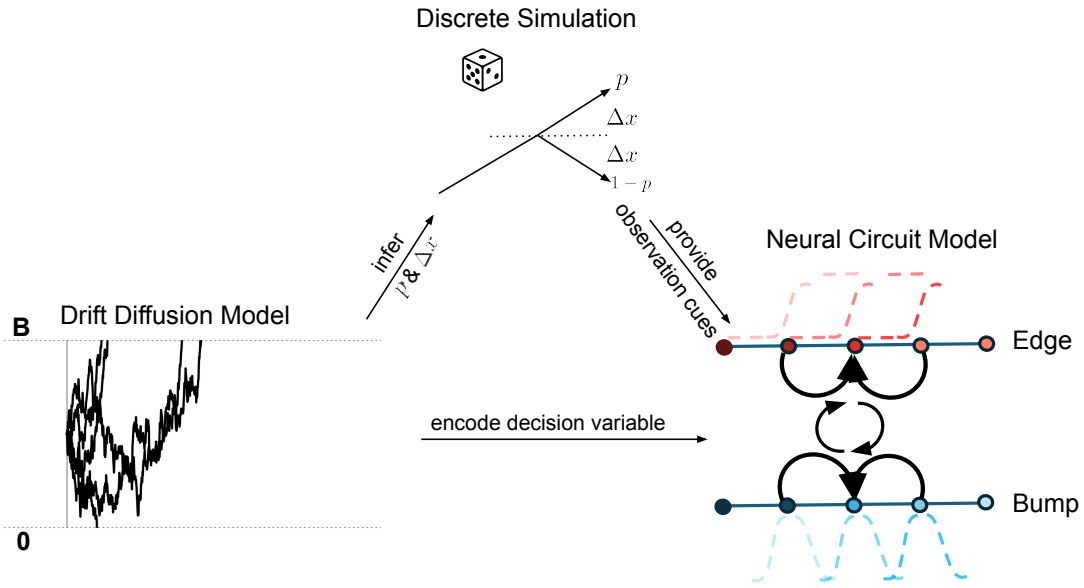

Figure 2: *Scheme of mapping a Drift diffusion model (DDM) onto our neural circuit model.* This figure provides the scheme to represent the decision variable in DDM via our neural circuit model. Given any drift rate A and noise scale σ_W, we use a discrete random walk simulation to approximate the continuous stochastic process by inferring the step size Δx and transition probability p. We thereby generate a series of observation cues for each trial provided to our neural circuit model.

Imagine we are given a drift rate A and noise scale σ_W, the first step is to convert it into a discrete Markov random walk by calculating the corresponding transition probability p and step size Δx. In the previous section we have shown that the moving speed v of the edge/bump attractor is linearly correlated with c_B. Thereby we can choose appropriate c_B such that the edge/bump attractor move exactly with the same speed as the decision variable moves along the evidence space,

$$c_B = \frac{\Delta x \sigma_1}{2h_B} \cdot \frac{\Delta t_{\text{DDM}}}{\Delta t_{\text{NN}}} \tag{30}$$

where Δt_{DDM} is the time interval between each two consecutive steps in discrete Markov random walk and Δt_{NN} is the time step of the neural network simulation. Finally, for each trial we generate a set of cue information $X_i \overset{\text{i.i.d.}}{\sim} \text{Bernoulli}(p)$, where p is the transition probability we calculated before. The cue information dynamically determines the sign of the feedback input from the bump attractor to the edge attractor, $I_{BE,D}(x,t)$. Consequently, at each time step the bump/edge attractor tends to shift by a distance Δx toward the direction favored by the cue, with probability p or $(1-p)$. Through this process, evidence is incrementally and precisely accumulated as the attractor traverses the evidence space.

3.2 Logarithmic evidence accumulation models in the Laplace domain

The last section provides a recipe to reproduce the standard DDM using our neural circuit model, in which c_B is chosen appropriately and assumed to be fixed over the trial. However, an edge/bump attractor with constant moving speed is not consistent with many neurophysiological evidence decision making tasks. Specifically, data suggests there are more sequentially firing neurons with receptive

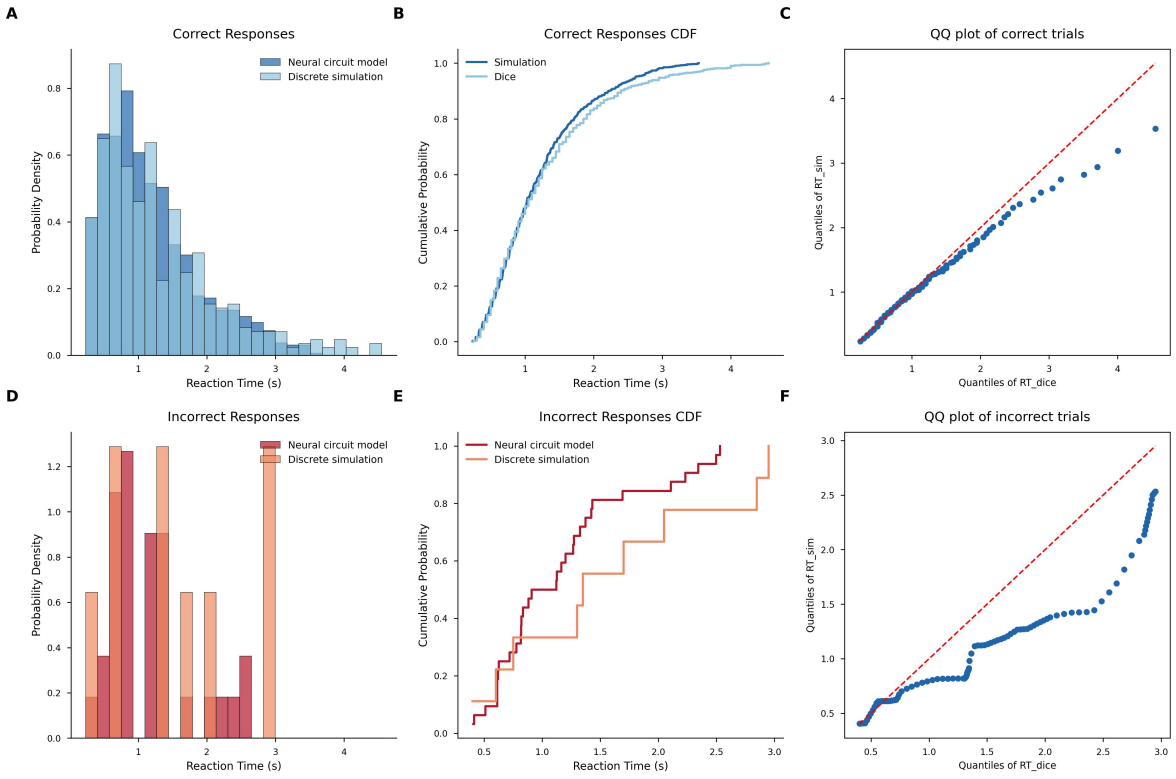

Figure 3: *Comparison of reaction time distribution between the discrete simulation of DDM and neural circuit model with inferred parameters.* In this simulation we set $A = 0.6$, $\sigma_W = 0.5$, $B = 0.8$, $\Delta t_{\text{DDM}} = 0.025s$, $\Delta t_{\text{NN}} = 0.001s$, $c_E = 0.5$. To infer c_B, we first conducted a series of simulations using a range of candidate c_B values, recording the corresponding edge speeds produced by the model. We then applied a linear fitting model to relate c_B to the resulting edge speed, and used this relationship to infer the value of c_B that would yield the theoretical edge speed predicted by the DDM parameters.

fields near the boundary and fewer with receptive fields further from the boundary, which results in a characteristic J-shaped pattern in the population activity heatmap. This is analogous to the sequential firing pattern of time cells where there are more neurons that fire early in the sequence and less neurons that fire later in the sequence. To account for this phenomenon, we assume c_B to be evidence-dependent so that the edge-bump attractor moves faster at an exponential scale when it approaches the decision boundary,

$$c_B(x) = c_0 \alpha^{-\beta(B-x)} \tag{31}$$

where c_0 controls the baseline connection strength, α controls the rate of exponential growth, β is a scaling factor, and B is the boundary value. The population activities of bump neurons show patterns of choice-selective sequence, with more right-preferred neurons when right decision is near to be reached and more left preferred neurons when left decision is near to be reached (Fig. 4A). The population activities of edge neurons show choice-selective ramping patterns with similar distribution of receptive fields (Fig. 4B). These together prove that the assumption of logarithmic evidence space is necessary for the neural circuit model to reproduce a non-uniform distribution of receptive fields in neurons.

3.3 Collapsing Boundary Model

Traditional DDM assumes a fixed boundary, i.e., the evidence accumulates until it reaches an amount of evidence a. a remains constant through out the time and serves as a parameter to be estimated from data. However, The fixed boundary model cannot explain a variety of data of decision making behavior of primate. For example, when thinking longer comes at an effort cost, a dynamical decision boundary

is optimal to account for the data. A traditional way to model the dynamical decision boundary is

$$u(t) = a - \left(1 - \exp\left(-(\frac{t}{\lambda})^k\right)\right)\left(\frac{1}{2}a - a'\right) \tag{32}$$

where a is the initial starting point of the boundary, a' is the asymptotic boundary setting, and λ and k are scaling and shape parameters.

To model a collapsing boundary in our neural circuit model, we define a scaling parameter

$$r(t) = \frac{u(t)}{B} \tag{33}$$

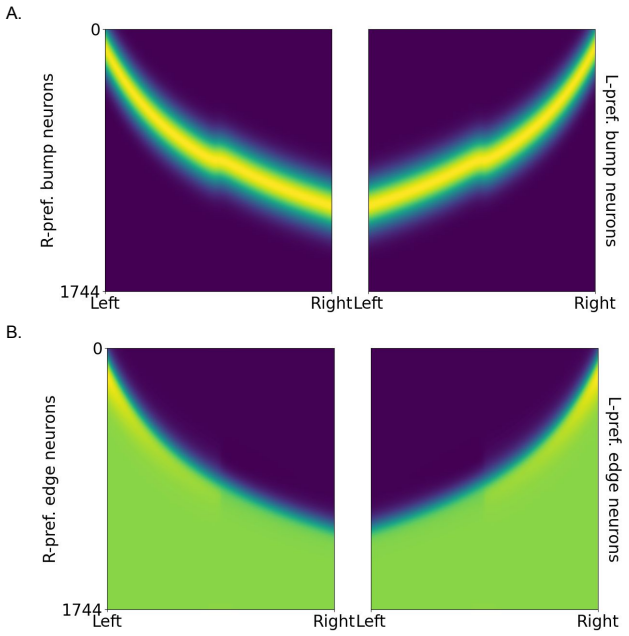

Figure 4: *Choice-selective sequential firing patterns and ramping firing patterns observed in the model simulation with the assumption of logarithmic evidence space.* On the top (Fig. 4A), the firing rate is shown as a function of evidence (confounded with time) when there is consistent evidence for the left cues. On the bottom (Fig. 4B), the activation is shown when there is consistent evidence for the right option.

and a rescaling decision variable

$$\tilde{x}(t) = \frac{x(t)}{r(t)} \tag{34}$$

Notice that when $x(t)$ hits the collapsing boundary $u(t)$, the rescaling decision variable $\tilde{x}(t)$ hits B. Thereby, we can reproduce the collapsing boundary model without the need of dynamically adjusting the decision boundary in our neural circuit model.

Rewriting the drift diffusion process about $\tilde{x}$ we have

$$d\tilde{x} = [A/r(t) - \tilde{x}\dot{r}(t)/r(t)]dt + c/r(t)dW \tag{35}$$

Similarly, we calculated the transition probability and the step size in our discrete approximation,

$$\begin{aligned} \Delta x(t) &= \frac{u(t)}{B}\Delta x_0 \\ p(t) &= \frac{1}{2}\left[1 + \frac{Adt}{\Delta x(t)}\right] \end{aligned} \tag{36}$$

where $\Delta x_0 = \sqrt{\sigma_W^2 dt + (Adt)^2}$. It is easy to verify that we still have

$$\begin{aligned} \mathbf{E}[\Delta x(t)] &= A dt \\ \mathrm{Var}[\Delta x(t)] &= \sigma_W^2 dt \end{aligned} \tag{37}$$

As time passes, the internal evidence increments become smaller but more strongly biased toward the preferred choice. This dual change reproduces the behavioural effect of a collapsing threshold: decision accuracy is maintained while mean reaction time shortens, matching empirical urgency phenomena in human and animal decision making.